

# Elasticity Detection: A Building Block for Delay-Sensitive Congestion Control

Prateesh Goyal, Akshay Narayan, Frank Cangialosi,  
Deepti Raghavan, Srinivas Narayana, Mohammad Alizadeh, Hari Balakrishnan  
MIT CSAIL

Email: nimbus@nms.csail.mit.edu

## ABSTRACT

This paper develops a technique to detect whether the cross traffic competing with a flow is elastic or not, and shows how to use the elasticity detector to improve congestion control. If the cross traffic is elastic, i.e., made up of buffer-filling flows like Cubic or Reno, then one should use a scheme that competes well with such traffic. Such a scheme will not be able to control delays because the cross traffic will not cooperate. If, however, cross traffic is inelastic, then one can use a suitable *delay-sensitive* congestion control algorithm, which can control delays, but which would have obtained dismal throughput when run concurrently with a buffer-filling algorithm.

We use the elasticity detector to demonstrate a congestion control framework that always achieves high utilization, but which can also achieve low delays when cross traffic permits it. The technique uses an asymmetric sinusoidal pulse pattern and estimates elasticity by computing the frequency response (FFT) of the cross traffic estimate; we have measured its accuracy to be over 90%. We have developed Nimbus, a protocol that explicitly switches between TCP-competitive and delay-sensitive modes using the elasticity detector. Our results on emulated and real-world paths show that Nimbus achieves throughput comparable to or better than Cubic always, but with delays that are much lower when cross traffic is inelastic. Unlike BBR, Nimbus is fair to Cubic, and has significantly lower delay in all cases; for example, on real-world paths, Nimbus has 11% lower throughput but at 40-50 ms lower packet delay.

## 1 INTRODUCTION

Popular congestion control algorithms such as Reno, Cubic, and Compound are *buffer-filling*; in the absence of an explicit signal of congestion from a router (packet loss or ECN), they increase their sending window (rate). It has long been recognized that such algorithms can cause excessive buffering and queuing delay in the network. Recently, there has been a resurgence of interest in this problem, because measurements have found “chronic overbuffering” [21], now termed “bufferbloat” [14], on many Internet paths.

Researchers have developed two categories of approaches to tackle bufferbloat: active queue management (AQM) and

delay-sensitive congestion control (DS) algorithms. AQM approaches [13, 17, 22, 31, 30] drop or mark packets before buffers fill up at routers; by providing earlier feedback of congestion to senders, buffer-filling senders can slow down before buffers fill. Because AQM schemes require changes to routers, however, they have faced deployment hurdles. By contrast, DS algorithms like Vegas [3], FAST [37], LEDBAT [32], Sprout [38], and Copa [1] require no router changes, using end-to-end delay and rate measurements to control queuing delay.

There is, however, a major practical obstacle to deploying *any* DS algorithm: their throughput is dismal when competing against buffer-filling algorithms at a shared bottleneck. The reason is that buffer-filling methods increase delays (until the router drops or marks packets); in response to increasing delays, a DS flow will keep reducing its rate, hoping to reduce delay. Throughput plummets, but delays don’t reduce; buffer-filling flows just grab more of the bottleneck.

Because the majority of traffic today on the Internet uses buffer-filling algorithms, it is hard to justify deploying a DS scheme on the Internet. In practice, algorithms like Compound [34] and BBR [6] that have been deployed use delay measurements (instead of, or in addition to, losses and ECN), but do not control delays. For example, Compound combines delay and loss measurements to grab bandwidth quickly, but it fills up buffers at its bottleneck and does not achieve low delay.

Is it possible to achieve the low delay of DS algorithms whenever possible, while ensuring that their throughput does not degrade in the presence of buffer-filling flows? In this paper, we present a new approach to congestion control that achieves this goal.

Our approach is based on the observation that only long-running backlogged flows running a buffer-filling algorithm tend to fill buffers. In the absence of packet loss, the rate of such flows increases to grab all available bandwidth. We call such flows *elastic*. By contrast, *inelastic* traffic—short flows, application-limited flows (e.g., a constant bit-rate video stream), or flows that are rate-limited—is not buffer-filling.

While DS algorithms suffer low throughput when cross traffic is elastic, they exhibit the desired behavior when cross traffic is inelastic: they achieve low delays while fully utilizing the bottleneck link. Therefore, if we can detect the presence

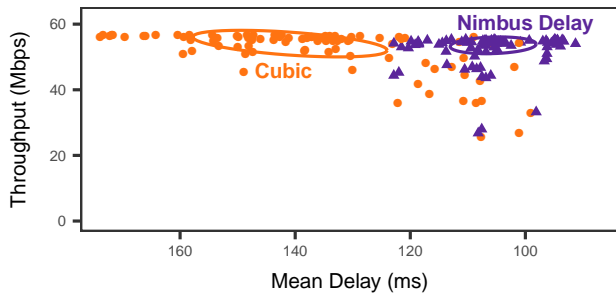


**Figure 1: Buffer-filling vs. delay-sensitive congestion control.** The plot shows the average throughput and delay for 100 experiments with Cubic and the Nimbus delay-control algorithm (§3). The experiments were run between a residential client (location redacted for anonymity) and an EC2 server in California. Each experiment lasted one minute.

of elastic TCPs, we can use a *TCP-competitive* algorithm (e.g., Cubic) to compete fairly with elastic flows when they appear, but switch to a DS algorithm when the cross traffic is inelastic. We call this approach *explicit mode switching*.

Our experiments on more than 25 Internet paths show that scenarios where cross traffic is predominantly inelastic are common. Figure 1 shows results from one of these paths. The plot shows the average throughput and average delay for Cubic and a DS scheme (described in §3) for 100 experiments with each protocol over a three-day period. Each experiment ran for 60 seconds. The DS scheme generally achieves much lower delays than Cubic, with similar throughput. This shows that there is an opportunity to significantly improve delays using DS algorithms, provided we can detect buffer-filling TCPs and compete with them fairly when needed.

Our main contribution is a new cross-traffic estimation technique (§2) to detect the presence of elastic flows using only end-to-end measurements. The insight behind this technique is that elastic and inelastic flows react differently to short-timescale traffic variations at the bottleneck link. The sender continuously modulates its rate to create small traffic fluctuations at the bottleneck at a specific frequency (e.g., 5 Hz). It concurrently monitors the rate of the cross traffic with a method we develop that uses only measurements at the sender. It checks the estimated cross traffic rate for signs that it is fluctuating at the same frequency. *If the cross traffic exhibits periodicity at the modulation frequency, the sender concludes that it is elastic; otherwise, it is inelastic.*

This technique works because the rate of an elastic flow changes with traffic fluctuations at the bottleneck link. The reason is that the packet transmissions of an elastic TCP flow are clocked by acknowledgements (“ACK-clocked”); therefore, fluctuations in the inter-packet arrival times at the receiver, which get reflected in ACKs, cause similar fluctuations in subsequent packet transmissions.

We have developed *Nimbus*, a congestion control protocol that uses the proposed elasticity detector to switch between a *delay-control mode* and a *TCP-competitive mode*. Fig. 2 shows an example result with Nimbus.

Explicit mode switching is a general technique; it can be applied to any combination of delay-sensitive and TCP-competitive congestion control algorithms. We demonstrate this by evaluating different variants of Nimbus that use Vegas [3], Copa [1], FAST [37], and our Nimbus delay-control method as DS algorithms, and Cubic, Reno [16], and MultTCP [8] as TCP-competitive algorithms.

Our cross traffic estimation technique requires some degree of traffic persistence. The sender must be able to create sufficient traffic variations and observe the impact on cross traffic over a period of time. Hence it is best suited for control of large flows, such as large file downloads, data backups to the cloud, etc. Fortunately, it is precisely for such transfers that delay-sensitive congestion control can provide the most benefit, since short flows are unlikely to cause bufferbloat [14].

We have implemented the elasticity detector and have experimented with it in the context of Nimbus with various DS and buffer-filling algorithms. Our implementation is in Linux using the recently proposed congestion control plane infrastructure [28]. Our experimental results include:

- (1) On an emulated bottleneck link (96 Mbit/s, 50 ms delay, 100 ms buffering) with a WAN cross-traffic trace, Nimbus achieves throughput comparable to BBR and Cubic but with a significantly smaller (50 ms) median delay.
- (2) Nimbus’s reduction in overall delays benefits the cross-traffic significantly: tail flow completion times for cross-traffic sharing the link with Nimbus are 3–4× smaller than with BBR both for short (< 15 KB) and long (> 150 MB) flows, and 1.25× smaller than Cubic for short flows.
- (3) Our elasticity detection method detects the presence of elastic cross-traffic correctly more than 90% of the time across a wide range of network characteristics such as cross-traffic RTTs, buffer size, Nimbus RTTs, bottleneck link rates, and the share of the bottleneck link rate controlled by Nimbus.
- (4) On Internet paths, Nimbus achieves throughput comparable to or better than Cubic on most of the 25 real-world paths we tested, with lower delays in 60% and the similar delays in the other 40% of paths. Compared to BBR, Nimbus achieves 10% lower mean throughput, but at 40-50 ms lower packet delay.

## 2 CROSS-TRAFFIC ESTIMATION

We first show how to estimate the total rate of cross traffic (§2.1) from measurements at the sender. Then, we show how to detect whether elastic flows are a significant contributor to

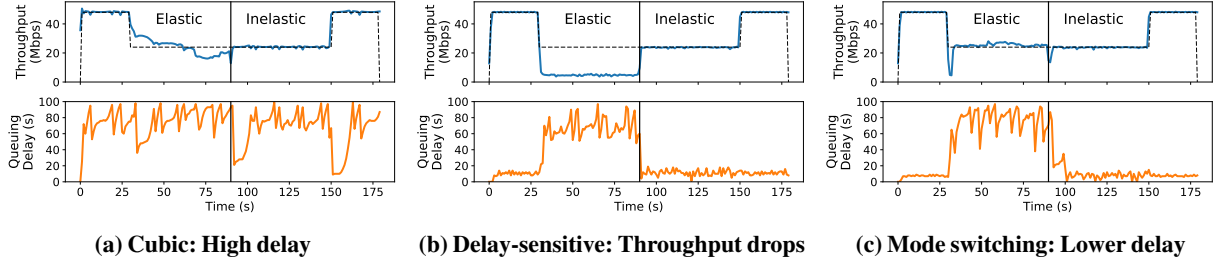


**Figure 2: Example of explicit mode switching.** In this experiment, we compare Cubic, a delay-sensitive algorithm (§3), and Nimbus, which uses explicit mode switching. In each experiment, the flow shares a 48 Mbit/s bottleneck link with one elastic long-running Cubic flow for 60 seconds (starting at  $t = 30$  sec.), followed by 60 seconds of inelastic traffic sending at 24 Mbit/s. Cubic has a large queuing delay throughout. The delay-sensitive scheme achieves low delay when the cross traffic is inelastic but suffers significant throughput loss when it competes with Cubic. Using explicit mode switching, Nimbus achieves the fair throughput against elastic traffic *and* low queuing delay when the cross traffic is inelastic.

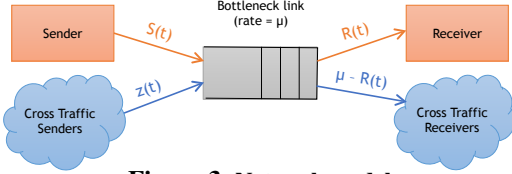


**Figure 3: Network model.**

the cross traffic, describing the key ideas (§2.2) and a practical method (§2.3).

Figure 3 shows the network model and introduces some notation. A sender communicates with a receiver over a *single* bottleneck link of rate  $\mu$ . The bottleneck link is shared with cross traffic, consisting of an unknown number of flows, each of which is either elastic or inelastic. A flow is elastic if three conditions hold: (i) its rate is limited by the TCP congestion window, (ii) its transmissions are ACK-clocked, and (iii) the congestion window increases on each ACK or every RTT as long as there is no indication of congestion. Otherwise, it is inelastic.  $S(t)$  and  $R(t)$  denote the time-varying sending and receiving rates, respectively, while  $z(t)$  is the total rate of the cross traffic. We assume that the sender knows  $\mu$ , and mention how to estimate it using prior work in §3.3.

## 2.1 Estimating the Rate of Cross Traffic

We estimate  $z(t)$  using the estimator

$$\hat{z}(t) = \mu \frac{S(t)}{R(t)} - S(t). \quad (1)$$

To understand why this estimator works, see Figure 3. The total traffic into the bottleneck queue is  $S(t) + z(t)$ , of which the receiver sees  $R(t)$ . As long as the bottleneck link is busy (i.e., its queue is not empty), and the router treats all traffic the same way, the ratio of  $R(t)$  to  $\mu$  must be equal to the ratio of  $S(t)$  and the total incoming traffic,  $S(t) + z(t)$ . Thus, any protocol that keeps the bottleneck link always busy can estimate  $z(t)$  using Eq. (1).

In practice, we can estimate  $S(t)$  and  $R(t)$  by considering  $n$  packets at a time:

$$S_{i,i+n} = \frac{n}{s_{i+n} - s_i}, \quad R_{i,i+n} = \frac{n}{r_{i+n} - r_i} \quad (2)$$

where  $s_k$  is the time at which the sender sends packet  $k$ ,  $r_k$  is the time at which the sender receives the ACK for packet  $k$ , and the units of the rate are packets per second. Note that measurements of  $S(t)$  and  $R(t)$  must be performed over the *same*  $n$  packets.

We have conducted several tests with various patterns of cross traffic to evaluate the effectiveness of this  $z(t)$  estimator. The overall error is small: the 50th and 95th percentiles of the relative error are 1.3% and 7.5%, respectively.

## 2.2 Elasticity Detection: Principles

We seek an online estimator to determine if the cross traffic includes elastic flows using only measurements at the sender.<sup>1</sup>

A strawman approach might attempt to detect elastic flows by estimating the contribution of the cross traffic to queuing delay. For example, the sender can estimate its own contribution to the queuing delay—i.e., the “self-inflicted” delay—and if the total queuing delay is significantly higher than the self-inflicted delay, conclude that the cross traffic is elastic.

This simple scheme does not work. To see why, consider again the experiment in Figure 2a, where a Cubic flow shares a link with both elastic and inelastic traffic in two separate time periods. Figure 4 plots the self-inflicted queuing delay for the Cubic flow in the same experiment. The self-inflicted delay looks nearly identical in the elastic and inelastic phases of the experiment. The reason is that a flow’s share of the queue occupancy is proportional to its throughput, independent of the elasticity of the cross traffic. This example suggests that no measurement at a single point in time can be used to reliably distinguish between elastic and inelastic cross traffic. In this

<sup>1</sup>Receiver modifications might improve accuracy by avoiding the need to estimate  $R(t)$  from ACKs at the sender, but would be a little harder to deploy.

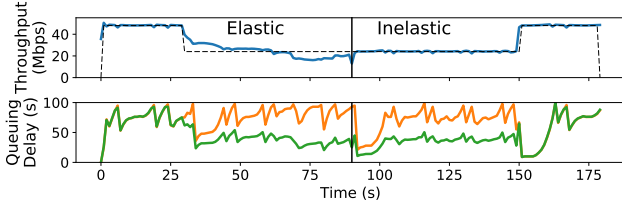


**Figure 4:** Delay measurements at a single point in time do not reveal elasticity. The bottom plot shows the total queuing delay (orange line) and the self-inflicted delay (green line). The experiment setup is the same as Figure 2a.

experiment, the Cubic flow gets roughly 50% of the bottleneck link; therefore, its self-inflicted delay is roughly half of the total queuing delay at all times.

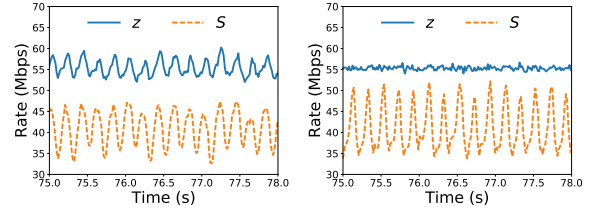
**To detect elasticity, tickle the cross traffic!** Our method detects elasticity by monitoring how the cross traffic responds to induced traffic variation at the bottleneck link over a period of time. The key observation is that elastic flows react in a predictable way to rate fluctuations at the bottleneck. Because elastic flows are ACK-clocked, if a new ACK is delayed by a time duration  $\delta$  seconds, then the next packet transmission will also be delayed by  $\delta$ . The sending rate depends on this delay: if the mean inter-arrival time between ACKs is  $d$ , adding an extra delay of  $\delta$  on each ACK would reduce the flow’s sending rate from  $1/d$  to  $1/(d+\delta)$  packets per second. By contrast, inelastic traffic does not respond like this to mild increases in delay.

We use this observation to detect elasticity by inducing changes in the inter-packet spacing of cross traffic at the bottleneck link. To achieve this, we transmit data in *pulses*, taking the desired sending rate,  $S(t)$ , and sending at a rate first higher, then lower than  $S(t)$ , while ensuring that the mean rate remains  $S(t)$ . Sending in such pulses (e.g., modulated on a sinusoid) modulates the inter-packet spacing of the cross traffic in the queue in a controlled way. If enough of the cross-traffic flows are elastic, then because of the explicitly induced changes in the ACK clocks of those flows, they will react to the changed inter-packet time. In particular, when we increase our rate and transmit a burst, the elastic cross traffic will reduce its rate in the next RTT; the opposite will happen when we decrease our rate.

Fig. 5a and Fig. 5b show the responses of elastic and inelastic cross-traffic flows ( $z$ ), when the sender transmits data in sinusoidal pulses ( $S(t)$ ) at frequency  $f_p = 5$  Hz. The elastic flow’s sending rate after one round-trip time of delay is inversely correlated with the pulses in the sending rate, while the inelastic flow’s sending rate is unaffected.

### 2.3 Elasticity Detection: Practice

To produce a practical method to detect cross traffic using this idea, we must address three challenges. First, pulses in our sending rate must induce a measurable change in  $z$ ,



(a) Elastic traffic

(b) Inelastic traffic

**Figure 5:** Cross traffic’s reaction to sinusoidal pulses. The pulses cause changes in the inter packet spacing for cross traffic. Elastic traffic reacts to these changes after a RTT. Inelastic cross traffic is agnostic to these changes.

but must not be so large as to congest the bottleneck link. Second, because there is natural variation in cross-traffic, as well as noise in the estimator of  $z$ , it is not easy to perform a robust comparison between the predicted change in  $z$  and the measured  $z$ . Third, because the sender does not know the RTTs of cross-traffic flows, it does not know when to look for the predicted response in the cross-traffic rate.

The first method we developed measured the *cross-correlation* between  $S(t)$  and  $z(t)$ . If the cross-correlation was close to zero, then the traffic would be considered inelastic, but a significant non-zero value would indicate elastic cross traffic. We found that this approach works well (with square-wave pulses) if the cross traffic is substantially elastic and has a similar RTT to the flow trying to detect elasticity, but not otherwise. The trouble is that cross traffic will react after its RTT, and thus we must align  $S(t)$  and  $z(t)$  using the cross traffic’s RTT, which is not easy to infer. Moreover, the elastic flows in the cross traffic may have different RTTs, making the alignment even more challenging, and rendering the method impractical.

**From time to frequency domain.** We have developed a method that overcomes the three challenges mentioned above. It uses two ideas. First, the sender modulates its packet transmissions using *sinusoidal pulses* at a known frequency  $f_p$ , with amplitude equal to a modest fraction (e.g., 25%) of the bottleneck link rate. These pulses induce a noticeable change in inter-packet times at the link without causing congestion, because the queues created in one part of the pulse are drained in the subsequent, and the period of the pulses is short (e.g.,  $f_p = 5$  Hz). By using short pulses, we ensure that the total burst of data sent in a pulse is a small fraction of the bottleneck’s queue size.

Second, the sender looks for periodicity in the cross-traffic rate at frequency  $f_p$ , using a frequency domain representation of the cross-traffic rates. We use the Fast Fourier Transform (FFT) of the time series of the cross traffic estimate  $z(t)$  over a short time interval (e.g., 5 seconds). Observing the cross-traffic’s response at a known frequency,  $f_p$ , yields a method that is robust to different RTTs in cross traffic.

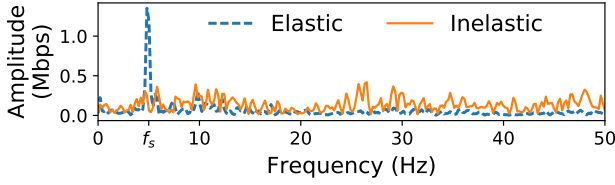


**Figure 6:** Cross traffic FFT for elastic and inelastic traffic. Only the FFT of elastic cross traffic has a pronounced peak at  $f_p$  (5 Hz).

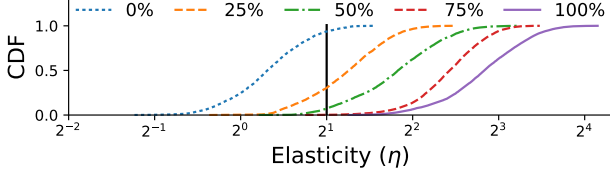


**Figure 7:** Distribution of elasticity with varying elastic fraction of cross traffic. Completely inelastic cross traffic has elasticity values close to zero, while completely elastic cross traffic exhibits high elasticity values. Cross traffic with some elastic fraction also exhibits high elasticity ( $\eta > 2$ ).

Fig. 6 shows the FFT of the  $z(t)$  time-series estimate produced using Eq. (1) for examples of elastic and inelastic cross traffic, respectively. Elastic cross traffic exhibits a pronounced peak at  $f_p$  compared to the neighboring frequencies, while for inelastic traffic the FFT magnitude is spread across many frequencies. The magnitude of the peak depends on how elastic the cross traffic is; for example, the more elastic the cross traffic, the sharper the peak at  $f_p$ .

Because the peak magnitude depends on the proportion of elastic flows in cross traffic, we found that a more robust indicator of elasticity is to compare the magnitude of the  $f_p$  peak to the next-best peak at nearby frequencies, rather than use a pre-determined absolute magnitude threshold. We define the *elasticity metric*,  $\eta$  as follows:

$$\eta = \frac{|FFT_z(f_p)|}{\max_{f \in (f_p, 2f_p)} |FFT_z(f)|} \quad (3)$$

Eq. (3) compares the magnitude of the FFT at frequency  $f_p$  to the peak magnitude in the range from just above  $f_p$  to just below  $2f_p$ . In Fig. 6,  $\eta$  for elastic traffic is 5, whereas for inelastic traffic it is close to 0.

In practice, the cross traffic is less likely to be either only elastic or only inelastic, but will be a mix. Fig. 7 shows elasticity of the cross traffic when we vary the percentage of bytes belonging to elastic flows in the cross traffic. Based on this data, we propose a hard-decision rule: if  $\eta \leq 2$ , then the cross traffic is considered inelastic; otherwise, it is elastic.

**Pulse shaping.** Rather than a pure sinusoid, we use an *asymmetric sinusoidal pulse*, as shown in Fig. 8. In the first

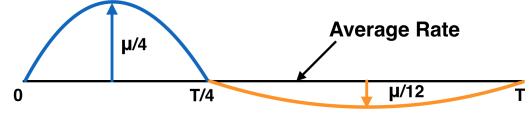


**Figure 8:** Example of an asymmetric sinusoidal pulse. The pulse has period  $T = 1/f_p$ . The positive half-sine lasts for  $T/4$  with amplitude  $\mu/4$ , and the negative half-sine lasts for the remaining duration, with amplitude  $\mu/12$ . The two half-sines are designed to cancel out each other over one period.

one-quarter of the pulse cycle, the sender adds a half-sine of a certain amplitude (e.g.,  $\mu/4$ ) to  $S(t)$ ; in the remaining three-quarters of the cycle, it subtracts a half-sine with one-third of the amplitude used in the first quarter of the cycle (e.g.,  $\mu/12$ ). The reason for this asymmetric pulse is that it enables senders with low sending rates,  $S(t)$ , to generate pulses. For example, for a peak amplitude of  $\mu/4$ , a sender with  $S(t)$  as low as  $\mu/12$  can generate the asymmetric pulse shown in Fig. 8; a symmetric pulse with the same peak rate would require  $S(t) > \mu/4$ . A peak pulse rate of  $\mu/4$  causes a noticeable change to inter-packet times by transmitting a fraction of BDP worth of packets over a short time period (less than an RTT).

What should the duration,  $T$ , of the pulse be? The answer depends on two factors: first, the duration over which  $S$  and  $R$  are measured (with which the sender estimates  $z$ ), and second, the amount of data we are able to send in excess of the mean rate without causing excessive congestion. If  $T$  were smaller than the measurement interval of  $S$  and  $R$ , then the pulse would have no measurable effect, because the excess in the high part and low part would cancel out over the measurement interval. But  $T$  cannot be too large because the sender sends in excess of the mean rate  $S(t)$  for  $T/4$ .

Based on these considerations, we set  $T$  so that  $T/4$  is on the order of the current RTT or a little less than that to avoid packet losses (e.g.,  $T/4$  could be the minimum observed RTT), and measure  $S$  and  $R$  (and hence,  $z$ ) using Eq. (2) over the duration of the current RTT (i.e., over exactly one window's worth of packets). As a concrete example, a flow with minimum RTT 50 ms would use  $T/4 = 50$  ms, giving a pulse frequency of  $1/0.2 = 5$  Hz.

In contrast to BBR's pulses, which are rectangular and probe the maximum delivery rate at the receiver (which may be thought of as a proxy for the bottleneck link rate,  $\mu$ ), our pulses are designed to produce an observable pattern in the FFT when the cross traffic is elastic. Using asymmetric sinusoidal pulses creates extra harmonics at multiples of the pulse frequency  $f_p$ . However, these harmonics do not affect the elasticity metric in Eq. (3), which only considers the FFT in the frequency band  $[f_p, 2f_p]$ .

### 3 NIMBUS: AN EXAMPLE PROTOCOL USING EXPLICIT MODE SWITCHING

This section describes a protocol that uses explicit mode switching. It has a TCP-competitive mode in which the sender transmits using Cubic’s congestion avoidance phase, and a delay-sensitive mode that uses a method, described below. The sender switches between the two modes using the elasticity detector described in the previous section, transmitting data at the time-varying rate dictated by the congestion control, and modulating its transmissions on the asymmetric sinusoid of Fig. 8.

#### 3.1 Delay-control Protocol

Nimbus uses a custom delay-sensitive control law inspired by ideas in XCP [20], TIMELY [27], and PIE [31]. It seeks to achieve high throughput while maintaining a specified threshold queueing delay,  $d_t > 0$ . A positive  $d_t$  ensures that the link is rarely under-utilized, and allows us to estimate  $z(t)$ . The protocol seeks to deliver an ideal rate of  $\mu - z(t)$ . The reason we designed our own method rather than use an existing one like Vegas [3] is because our ability to estimate  $z$  yields tighter controls on delay than prior protocols.

The control rule has two terms. The first seeks to achieve the ideal rate,  $\mu - z$ . The second seeks to maintain a specified threshold queueing delay,  $d_t$ , to prevent the queue from both emptying and growing too large.

Denote the minimum RTT by  $x_{\min}$  and the current RTT by  $x_t$ . The Nimbus delay-control rule is

$$S(t+\delta) = (1-\alpha)S(t) + \alpha(\mu - z(t)) + \beta \frac{\mu}{x_t}(x_{\min} + d_t - x_t). \quad (4)$$

Prior work (XCP [20] and RCP [2]) has established stability bounds on  $\alpha$  and  $\beta$  for nearly identical control laws. Our implementation uses  $\alpha = 0.8$ , and  $\beta = 0.5$ .

#### 3.2 Mode Switching

Nimbus uses the pulsing parameters described in §2.3, calculating  $S$  and  $R$  over one window’s worth of packets and setting  $T/4$  to the minimum RTT. It computes the FFT over multiple pulses and uses the  $z$  measurements reported in the last 5 seconds to calculate elasticity ( $\eta$ ) using Eq. (3).

We found earlier (Fig. 7) that a good threshold for  $\eta$  is 2. To prevent frequent mode switches, Nimbus applies a hysteresis to this threshold before switching modes. When in delay-sensitive mode,  $\eta$  must exceed 2.25 to switch to TCP-competitive mode, and when in TCP-competitive mode,  $\eta$  must be lower than 2 to switch to delay-sensitive mode.

It is important that the rate be initialized carefully on a mode switch. When switching to TCP-competitive mode, Nimbus sets the rate (and equivalent window) after switching to the rate that was being used five seconds ago (five seconds is the duration over which we calculate the FFT). The reason is that the elasticity detector takes five seconds to detect the presence

of elastic cross traffic, and the arrival of elastic traffic over the past five seconds would have reduced the delay mode’s rate. We set the new congestion window to the inflection point of the Cubic function, so the rate over the next few RTTs will rise faster in each successive RTT, and we reset `ssthresh` to this congestion window to avoid entering slow start.

While switching to delay mode, Nimbus resets the delay threshold to the current value of  $x_t - x_{\min}$ , rather than to the desired threshold  $d_t$ , and linearly decreases the threshold used in the control rule to the desired  $d_t$  over several RTTs. The reason is that  $x_t - x_{\min}$  is likely to have grown much larger than  $d_t$  in TCP-competitive mode, and using  $d_t$  would only cause the sender to reduce its rate and go down in throughput. The approach we use ensures instead that the delay mode will drain the queues gradually and won’t lose throughput instantly, and also provides a safeguard against incorrect switches to delay mode.

#### 3.3 Implementation

We implemented Nimbus using the congestion control plane (CCP) [28, 7], which provides a convenient way to express the signal processing operations in user-space code while achieving high rates. The implementation runs at up to 40 Gbit/s using the Linux TCP datapath. All the Nimbus software is in user-space. The Linux TCP datapath uses a CCP library to report to our Nimbus implementation the estimates of  $S$ ,  $R$ , the RTT, and packet losses every 10 ms.  $S$  and  $R$  are measured using the methods built in TCP BBR over one window’s worth of packets. Our implementation of Nimbus is rate-based, and sets a cap on the congestion window to prevent uncontrolled “open-loop” behavior when ACKs stop arriving.

On every measurement report, Nimbus (1) updates the congestion control variables of the current mode and calculates a pre-pulsing sending rate, (2) superimposes the asymmetric pulse in Fig. 8 to obtain the actual sending rate, and (3) generates the FFT of  $z$  and makes a decision to switch modes using a 5-second measurement period for the FFT.

We note that calculating  $z$  requires an estimate of the bottleneck link rate ( $\mu$ ). There has been much prior work [18, 10, 11, 23, 19, 24, 25] in estimating  $\mu$ , any of which could be incorporated in Nimbus. Like BBR, our current implementation uses the maximum received rate, taking care to avoid incorrect estimates due to ACK compression and dilation.

#### 3.4 Visualizing Nimbus and Other Schemes

We illustrate Nimbus on a synthetic workload with time-varying cross traffic. We emulate a bottleneck link in Mahimahi [29], a link emulator.

The network has a bottleneck link rate of 96 Mbit/s, a minimum RTT of 50 ms, and 100 ms (2 BDP) of router buffering. Nimbus sets a target queueing delay threshold of 12.5 ms in

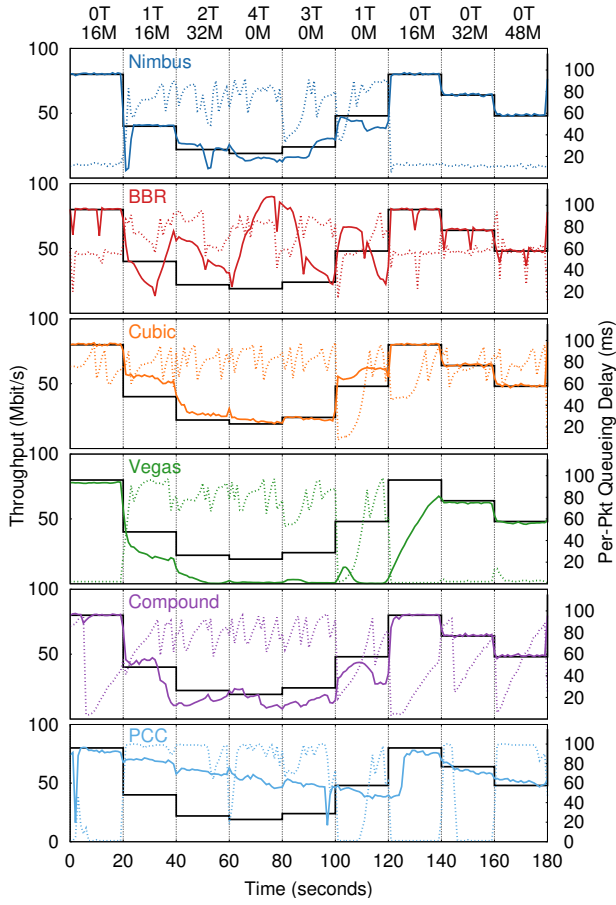


**Figure 9: Performance on a 96 Mbit/s Mahimahi link with 50 ms delay and 2 BDP of buffering while varying the rate and type of cross traffic as denoted at the top of the graph.  $xM$  denotes  $x$  Mbit/s of inelastic Poisson cross-traffic.  $yT$  denotes  $y$  long-running Cubic cross-flows. The solid black line indicates the correct time-varying fair-share rate that the protocol should achieve given the cross-traffic. By switching modes, Nimbus both competes fairly with elastic traffic and utilizes all available spare capacity with low delays against inelastic traffic.**

delay-sensitive mode. We compare Nimbus with Linux implementations of Cubic, BBR [6], and Vegas [3], our empirically-validated implementation of Compound [34] in atop CCP [28, 7], and the PCC-authors’ implementation of PCC [9].

The cross-traffic type varies over time between elastic, inelastic, and a mix of the two. We generate inelastic cross-traffic using a simple custom traffic generator, with packet transmissions generated as a Poisson process with a fixed mean rate. Elastic cross-traffic uses TCP Cubic. We generate all elastic traffic (Nimbus and cross-traffic) using `iperf` [35]. Mahimahi provides received throughput (over one second) and queueing delays (per packet) for all algorithms.

Fig. 9 shows the receiver throughput and queueing delays for the various algorithms, as well as the correct fair-share rate over time. Throughout the experiment, Nimbus achieves both its fair share rate and low ( $\leq 20$  ms) queueing delays in the presence of inelastic cross-traffic. With elastic cross-traffic, Nimbus switches to competitive mode within 5 s and achieves close to its fair-share rate. The delays during this period approach the buffer size because the competing traffic is buffer-filling; the delays return to their previous low value (20 ms) within 5 s after the elastic cross-flows complete.

We find that the other algorithms suffer either from higher queueing delays or unfair throughput. Cubic experiences high delays close to the buffer size (100 ms) throughout the experiment.

BBR attains throughput that is often *significantly higher* than its fair share and suffers from high delays even with inelastic cross-traffic; this is consistent with a prior result [1]. BBR’s principle of setting its sending traffic to the estimated link rate is problematic in the presence of any cross-traffic. Further, its use of the maximum achieved delivery rate as the “right” sending rate has been shown [15] to cause BBR to unnecessarily inflate queueing delays.

Vegas suffers from low throughput in the presence of elastic cross-traffic, as it reduces its sending rate in the presence of large delays. Compound ramps up its rate quickly whenever it detects low delays, but behaves like TCP Reno otherwise. Consequently, it attains its fair-share rate, but suffers from high delays even with inelastic cross-traffic.

PCC optimizes delivery rates using an online objective function, but this local optimization results in significant unfairness to TCP cross-traffic as well as high queueing delays.

## 4 MULTIPLE NIMBUS FLOWS

What happens when a bottleneck is shared by multiple Nimbus flows running on different senders? The goal is for all the Nimbus flows to remain in delay-sensitive mode when there is no other elastic cross traffic, and compete well with elastic cross traffic otherwise. The problem is that pulsing may create adverse interactions that confuse the different Nimbus instances.

One approach is for the Nimbus flows to all pulse at the same frequency. However, in this case, they will all detect a peak in the FFT at the oscillation frequency. They will all then stay in TCP-competitive mode and won’t be able to maintain low delays, even when there is no elastic cross traffic. A second approach is for different Nimbus flows to pulse at different frequencies. The problem with this approach is that it cannot scale to more than a few flows, because the set of possible frequencies is too small (recall that we require  $T/4 \approx RTT$ ).

**Watchers, meet Pulser.** We propose a third approach. One of the Nimbus flows assumes the role of the *pulser*, while the others are *watchers*. The coordination between them involves

no explicit communication; in fact, each Nimbus flow is unaware of the identities, or even existence, of the others.

The pulser sends data by modulating its transmissions on the asymmetric sinusoid. The pulser uses two different frequencies,  $f_{pc}$  in TCP-competitive mode, and  $f_{pd}$  in delay-sensitive mode; e.g., 5 Hz and 6 Hz. The values of these frequencies are fixed and agreed upon beforehand. A watcher infers whether the pulser is pulsing at frequency  $f_{pc}$  or frequency  $f_{pd}$  by observing the FFT at those two frequencies and uses it to set its own mode to match the pulser’s mode. The variation in the queueing due to pulsing will cause a watcher flow’s receive rate to pulse at the same frequency. The watcher computes the FFT at the two possible pulsing frequencies and picks the mode corresponding to the larger value. With this method, a watcher flow can determine the mode without estimating the bottleneck link rate or controlling a significant portion of the link rate.

For multiple Nimbus flows to maintain low delays during times when there is no elastic cross traffic on the link, the pulser flow must classify watcher traffic as inelastic. Note that from the pulser’s perspective, the watchers flows are part of the cross traffic; thus, to avoid confusing the pulser, the rate of watchers must not react to the pulses of the pulser. To achieve this goal, a watcher applies a low pass filter to its transmission rate before sending data. The low pass filter cuts off all frequencies in the sending rate that exceed  $\min(f_{pc}, f_{pd})$ .

**Pulser election.** A decentralized and randomized election process decides which flow is the pulser and which are watchers. If a Nimbus flow determines that there is no pulser (by seeing that there is no peak in the FFT at the two potential pulsing frequencies), then it decides to become a pulser with a probability proportional to its transmission rate:

$$p_i = \frac{\kappa \tau}{\text{FFT Duration}} \times \frac{R_i}{\hat{\mu}_i}. \quad (5)$$

Each flow makes decisions periodically, e.g., every  $\tau = 10$  ms, and  $\kappa$  is a constant. Since the FFT duration is 5 seconds, each  $p_i$  is small (note that  $\sum_i R_i \leq \mu$ ), but since flows make decisions every  $\tau$  seconds, eventually one will become a pulser.

If the estimates  $\hat{\mu}_i$  are equal to the true bottleneck rate  $\mu$ , then the expected number of flows that become pulsers over the FFT duration is at most  $\kappa$ . To see why, note that the expected number of pulsers is equal to the sum of the probabilities in Eq. (5) over all the decisions made by all flows in the FFT duration. Since  $\sum_i R_i \leq \mu$  and each flow makes (FFT Duration/ $\tau$ ) decisions, these probabilities sum up to at most  $\kappa$ .

It is also not difficult to show the number of pulsers within an FFT duration has approximately a Poisson distribution with a mean of  $\kappa$  [12]. Thus the probability that after one flow becomes a pulser, a second flow also becomes a pulser before it can detect the pulses of the first flow in its FFT measurements is  $1 - e^{-\kappa}$ . Therefore,  $\kappa$  controls the tradeoff between fewer conflicts vs. longer time to elect a pulser.

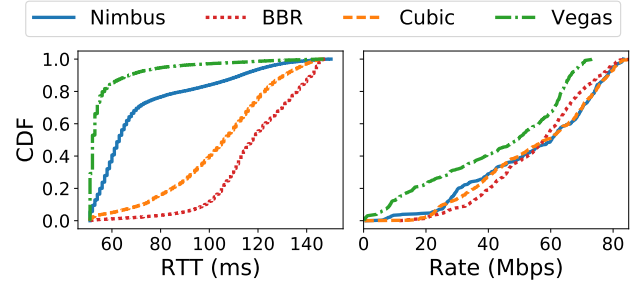


**Figure 10: Nimbus reduces delay relative to Cubic and BBR while achieving comparable throughput on a cross-traffic workload derived from a packet trace collected at a WAN router.**

For any value of  $\kappa$ , there is a non-zero probability of more than one concurrent pulser. If there are multiple pulsers, then each pulser will observe that the cross traffic has more variation than the variations it creates with its pulses. This can be detected by comparing the magnitude of the FFT of the cross traffic  $z(t)$  at  $f_p$  with the FFT of the pulser’s receive rate  $R(t)$  at  $f_p$ . If the cross traffic’s FFT has a larger magnitude at  $f_p$ , Nimbus concludes that there must be multiple pulsers and switches to a watcher with a fixed probability.

## 5 EVALUATION

We answer the following questions in this section.

- §5.1: Does Nimbus achieve low delay and high throughput?
- §5.2: Conversely, does switching help cross-traffic?
- §5.3: Does Nimbus need to control a large link share?
- §5.4: Does the elasticity detector track the elastic fraction?
- §5.5: How robust is Nimbus’s elasticity detection?
- §5.6: Can multiple Nimbus flows co-exist well?
- §5.7: Does Nimbus perform well on real Internet paths?
- §5.8: Can we use other DS and buffer-filling algorithms?

We evaluate the elasticity detection method and Nimbus using the Mahimahi emulator with realistic workloads, and on Internet paths. Our Internet experiments are over paths between Amazon’s EC2 machines around the world, well-connected university networks, and residential hosts.

### 5.1 Does Nimbus Achieve Low Delays and High Throughput?

We evaluate the delay and throughput benefits of explicit mode-switching using a trace-driven emulation. We generate cross-traffic from an empirical distribution of flow sizes derived from a wide-area packet trace from CAIDA [4]. This packet trace was collected at an Internet backbone router on January 21, 2016 and contains over 30 million packets recorded over 60 seconds. The maximum rate observed over any 100 ms period is 2.2 Gbit/s. We generate Cubic cross-flows

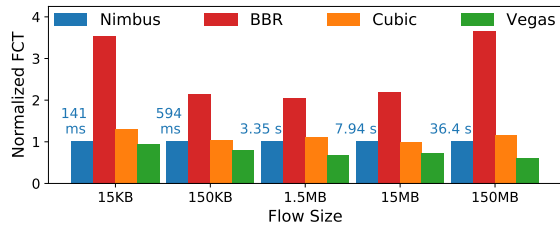


**Figure 11: Using Nimbus reduces the p95 FCT of cross-flows relative to BBR at all flow sizes, and relative to Cubic for short flows. Vegas provides low cross-flow FCT, but its own rate is low.**

with flow sizes drawn from this data, with flow arrival times generated by a Poisson process to offer a fixed average load.

One backlogged flow running a fixed algorithm (Nimbus, Cubic, Vegas, or BBR) and the WAN-like cross-flows share a 96 Mbit/s Mahimahi bottleneck link with a propagation round-trip time of 50 ms and a bottleneck buffer of 100 ms. We generate cross-traffic to fill 50% link load (48 Mbit/s) on average. Nimbus uses a queueing delay threshold of 12.5 ms in delay-mode and emulates Cubic in competitive-mode.

Fig. 10 shows the throughput and packet delays of Nimbus, Vegas, Cubic, and BBR. Nimbus achieves a throughput distribution comparable to Cubic and BBR, while Vegas suffers from low throughput. Unlike Cubic and BBR, however, Nimbus also achieves low RTTs, with a median only 10 ms higher than Vegas and  $> 50$  ms lower than Cubic and BBR. Because of explicit mode-switching, Nimbus is the only algorithm to achieve low delays comparable to Vegas with the high throughput of Cubic.

## 5.2 Does Switching Help Cross-Traffic?

Using the same setup as §5.1, we measure the flow completion time (FCT) of cross-flows. Fig. 11 compares the 95th percentile (p95) cross-flow FCT for cross-flows of different sizes. The FCTs are normalized by the corresponding value for Nimbus at each flow size.

BBR exhibits much higher cross-flow FCT at all sizes compared to all the other protocols, consistent with the observation of unfairness §3.4. For small cross-flows (15 KB or less), the p95 FCT for Nimbus is comparable to Vegas and lower than Cubic. With Nimbus p95 FCT of cross traffic at higher flow sizes are slightly lower than Cubic because of small delays in switching to TCP-competitive-mode. At all flow sizes, Vegas provides the best cross-flow FCTs, but its own flow rate is dismal (§5.1).

## 5.3 Does Nimbus Need to Control a Large Link Share?

Must Nimbus control a significant fraction of the link rate to reap the benefits of explicit mode-switching? We evaluate Nimbus’s delay and throughput relative to other algorithms when Nimbus controls varying shares of the link rate. We

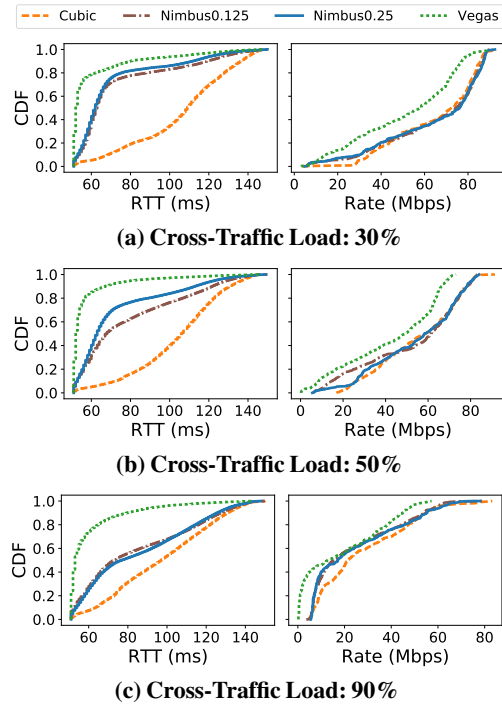


**Figure 12: At low cross-traffic loads, Nimbus’s queueing delay approaches that of Vegas while its throughput approaches that of Cubic. At high loads, Nimbus behaves like Cubic. Increasing pulse size improves switching accuracy and performance.**

generate cross-traffic as described in §5.1 but vary the offered load of the cross-traffic at three levels (30%, 50%, and 90% of the link rate). We measure throughput and delay for two pulse sizes:  $0.125\mu$  and  $0.25\mu$ .

Fig. 12 shows our findings. First, in all cases, Nimbus lowers delay without hurting throughput, with the delay benefits most pronounced when cross traffic is low. Second, as cross traffic increases, Nimbus’s delay improvements decrease, because it must stay in TCP-competitive mode more often. Third, Nimbus’s behavior is better at the larger pulse size, but its benefits are generally robust even at  $0.125\mu$ .

Elasticity detection is less accurate with smaller pulse amplitude ( $0.125\mu$ ), causing more errors in mode-switching. With this pulse size, Nimbus does not lower its delays or maintain its throughput as effectively at medium load (50%) when switching correctly matters more for good performance.

In the next two sections, we evaluate the applicability of Nimbus’s elasticity detection method to real workloads, and test the method’s robustness to various network-level characteristics.

## 5.4 Does $\eta$ Track the True Elastic Fraction?

We use the setup of §5.1 to present a mix of elastic and inelastic cross traffic, and evaluate how well the detector’s decision

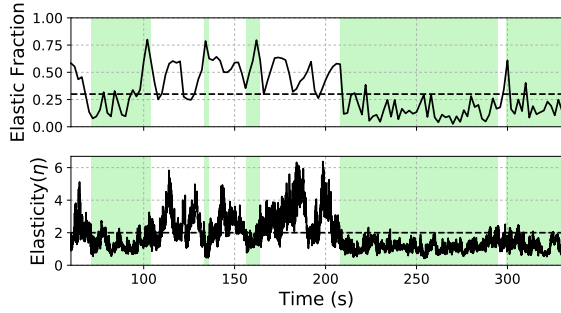


**Figure 13: Elasticity metric for realistic cross-traffic (§5.4)—** The elasticity metric, and hence Nimbus’s mode, closely tracks the prevalence of elastic cross-traffic (ground truth measured independently using the volume of ACK-clocked flows). Green-shaded regions indicate inelastic periods.

correlates with the true proportion of elastic traffic. We define a cross-flow generated from the CAIDA trace as “elastic” if it is guaranteed to have ACK-clocked packet transmissions over its lifetime, i.e., flows with sizes higher than TCP’s default initial congestion window (10 packets in Linux 4.10, which is our transmitter).

The top chart in Fig. 13 shows the fraction of bytes belonging to elastic flows as a function of time. The bottom chart shows the output of the elasticity detector along with the dashed threshold line at  $\eta = 2$ . The green shaded regions are times when Nimbus was in delay-sensitive mode. These correlate well with the times when the elastic fraction was low; when the elasticity fraction is  $< 0.3$ , the elasticity detector correctly outputs “inelastic” over 90% of the time, when one accounts for the 5 second estimation delay. Even counting that delay, the accuracy is over 80%.

## 5.5 How Robust is Elasticity Detection?

We now evaluate the robustness of our elasticity detection method to cross-traffic and Nimbus’s RTTs, bottleneck link rate, the share of the bottleneck controlled by Nimbus, bottleneck buffer size, and Nimbus’s pulse size. Unless specified otherwise, we run Nimbus as a backlogged flow on a 96 Mbit/s bottleneck link with a 50 ms propagation delay and a 100 ms drop-tail buffer (2 BDP). We supply Nimbus with the correct link rate for these experiments, allowing us to study the robustness of elasticity detection with respect to the properties mentioned above. We consider three categories of synthetic cross-traffic sharing the link with Nimbus: (i) fully inelastic traffic (Poisson); (ii) fully elastic traffic (backlogged NewReno flows); and (iii) an equal mix of inelastic and elastic. The duration of each experiment is 120 seconds. The main performance metric is *accuracy*: the fraction of time that Nimbus correctly detects the presence of elastic cross-traffic.

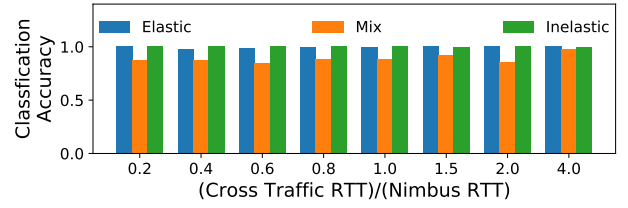


**Figure 14: Nimbus classifies purely elastic and inelastic traffic with accuracy greater than 98%. For a mix of elastic and inelastic traffic, the average accuracy is greater than 80% in all cases.**

**Impact of cross-traffic RTT.** We vary the cross-traffic’s propagation round-trip time from 10 ms ( $0.2\times$  that of Nimbus) to 200 ms ( $4\times$  that of Nimbus). Fig. 14 shows the mean accuracy across 5 runs of each category of cross-traffic. We find that varying cross-traffic RTT does not impact detection accuracy. For purely inelastic and purely elastic traffic, Nimbus achieves an average accuracy of more than 98% in all cases, while for mixed traffic, Nimbus achieves a mean accuracy of 80% in all cases (a random guess would’ve achieved only 50%).

**Impact of pulse size, link rate, and link share controlled by Nimbus.** We perform a multi-factor experiment varying Nimbus’s pulse size from  $0.0625\times$ — $0.5\times$  the link rate, Nimbus’s fair share of the bottleneck link rate from 12.5%—75%, and bottleneck link rates set to 96, 192, and 384 Mbit/s. The accuracy for purely elastic cross-traffic was always higher than 95%.

Fig. 15 shows the average detection accuracy over five runs of the other two categories of cross-traffic. Nimbus achieves an accuracy of more than 90% averaged over all the points. In general, increasing the pulse sizes improves accuracy because Nimbus can create a more easily observable change in the cross-traffic sending rates. An increase in the link rate results in higher accuracy for a given pulse size and Nimbus link share because the variance in the rates of inelastic Poisson cross-traffic reduces with increasing cross-traffic sending rate, reducing the number of false peaks in the cross-traffic FFT. For the same reason, decreasing Nimbus’s share of the link also results in higher accuracy in general. However, at low link rates, Nimbus has low accuracy ( $\sim 60\%$ ) when it uses high pulse sizes and controls a low fraction of the link rate. We believe that this is due to a quirk in the way the Linux networking stack reports round-trip time measurements under sudden sending rate changes.

**Impact of buffer size and RTT.** We vary the buffer size from 0.25 BDP to 4 BDP for each category of cross traffic, at propagation round-trip times of 25 ms, 50 ms, and 75 ms. With purely elastic or inelastic traffic, Nimbus has an average accuracy (across 5 runs) of 98% or more in all cases but one (see below), while with mixed traffic, the accuracy is always 85% or more. With shallow buffers, when the buffer

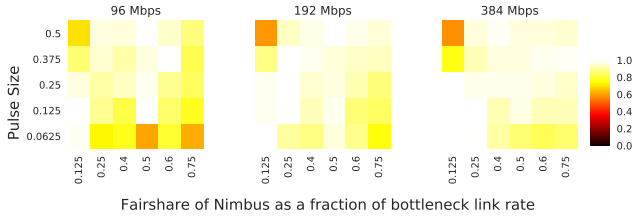


**Figure 15: Nimbus is robust to variations in link bandwidth and fraction of traffic controlled by it. Increasing pulse size increases robustness.**

size is less than the product of the delay threshold  $x_t$  and the bottleneck link rate (i.e., 0.25 BDP when the round-trip time is 50 ms), Nimbus classifies all traffic as elastic. However, this low accuracy does not impact the performance of Nimbus, as Nimbus achieves its fair-share throughput and low delays (bounded by the small buffer size). Further, accuracy decreases when Nimbus’s RTT exceeds its pulse period. Since Nimbus’s measurements of rates are over one RTT, any oscillations over a smaller period are hard to observe.

## 5.6 Can Multiple Nimbus Flows Co-Exist?

Does explicit mode-switching permit low delays in the presence of multiple mode-switching flows (and possibly other cross-traffic)? Can multiple such flows share a bottleneck link fairly with each other and with cross-traffic? We run Nimbus with Vegas as its delay-mode algorithm and supply it with the correct link rate. (We use Vegas because Nimbus’s rule in its present form is not fair to other flows with the same rule.)

Fig. 16 demonstrates how Nimbus flows react as other Nimbus flows arrive and leave (there is no other cross-traffic). Four flows arrive at a link with rate 96 Mbit/s and round-trip time 50 ms. Each flow begins 120 s after the last one began, and lasts for 480 s. The top half shows the rates achieved by the four flows over time. Each new flow begins as a watcher. If the new flow detects a pulser ( $t = 120, 240, 360$  s), it remains a watcher. If the pulser goes away or a new flow fails to detect a pulser, one of the watchers becomes a pulser ( $t = 480, 720$  s). The pulser can be identified visually by its rate variations.

The flows share the link rate equally. The bottom half of the figure shows the achieved delays with red background shading to indicate when one of the flows is (incorrectly) in competitive-mode. The flows maintain low RTTs and stay in delay-mode for most of the time.

Fig. 17 demonstrates multiple Nimbus flows switching in the presence of cross-traffic. We run three Nimbus flows on an emulated 192 Mbit/s link with a propagation delay of 50 ms. The cross traffic is synthetic. In the first 90 s, the cross-traffic is elastic (three Cubic flows), and for the rest of the experiment, the cross-traffic is inelastic (96 Mbit/s constant bit-rate). The top graph shows the total rate of the three Nimbus flows, along

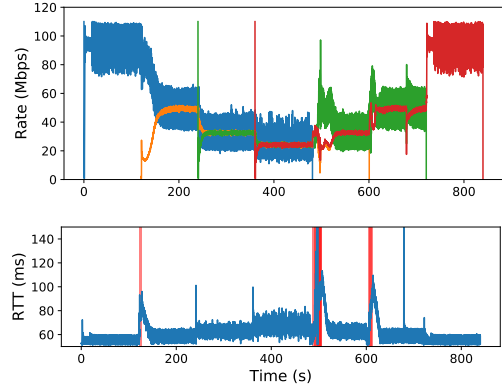


**Figure 16: Multiple Nimbus flows achieve fair sharing of a bottleneck link (top graph). There is at most one pulser flow at any time, which can be identified by its rate variations. Together, the flows achieve low delays by staying in delay mode for most of the duration (bottom graph). The red background shading shows when a Nimbus flow was (incorrectly) in competitive mode.**

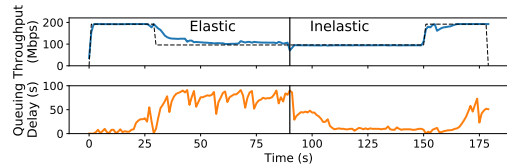


**Figure 17: Multiple Nimbus flows and other cross-traffic (§5.6)— There are 3 Nimbus flows throughout. Cross traffic in the first 90 s is elastic and made up of three Cubic flows. Cross traffic in the rest of the experiment is inelastic and made up of a 96 Mbit/s constant bit-rate stream. Multiple Nimbus flows achieve their fair share rate (top) while maintaining low delays in the absence of elastic cross traffic (bottom).**

with a reference line for the fair-share rate of the aggregate. The graph at the bottom shows the measured queueing delays. Nimbus shares the link fairly with other cross-traffic, and achieves low delays by staying in the delay mode in the absence of elastic cross-traffic.

## 5.7 Real-World Internet Paths

We ran Nimbus on the public Internet with a test-bed of five servers and five clients, 25 paths in all. The servers are Amazon EC2 instances located in California, London, Frankfurt, Ireland, and Paris, and are rated for 10 Gbit/s. We verified that the bottleneck in each case was not the server’s Internet link. We use five residential hosts in different ASes as clients. On each path, we initiate bulk data transfers using Nimbus, Cubic, BBR, and Vegas. We run one minute experiments over five hours on each path, and measure the achieved average throughput and mean delay.

Fig. 18 shows throughput and delays over three of the paths. The  $x$  (delay) axis is inverted; better performance is up and to

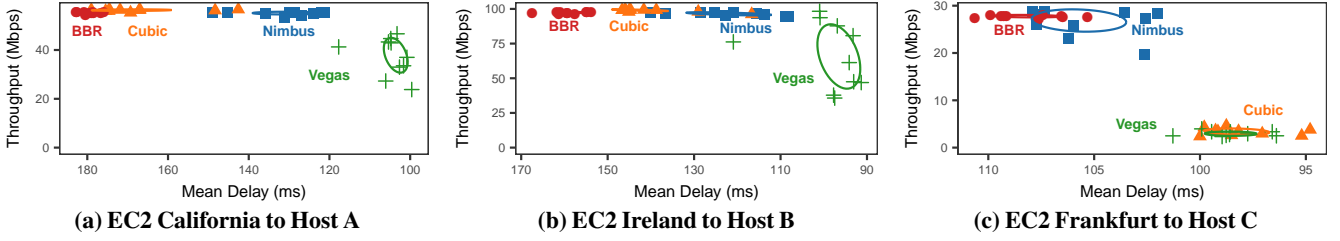


**Figure 18: Performance on three example Internet paths (§5.7).** The  $x$  axis is inverted; better performance is up and to the right. On paths with buffering and no drops, ((a) and (b)), Nimbus achieves the same throughput as BBR and Cubic but reduces delays significantly. On paths with significant packet drops (c), Cubic suffers but Nimbus achieves high throughput.

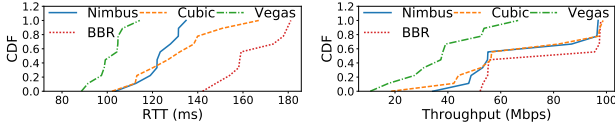


**Figure 19: CDF of Rate and RTT on real-world paths with queueing.** Nimbus reduces the RTT compared to Cubic and BBR (40-50 ms lower), at similar throughput.

the right. We find that Nimbus achieves high throughput comparable to BBR in all cases, at noticeably lower delays. Cubic attains high throughput on paths with deep buffers (Fig. 18a and Fig. 18b), but not on paths with packet drops or policers (Fig. 18c). Vegas attains poor throughput on these paths due to its inability to compete with elastic cross-traffic. These trends illustrate the utility of explicit mode-switching on Internet paths: it is possible to achieve high throughput and low delays over the Internet using delay-sensitive algorithms with the ability to switch to a different competitive mode when required.

Fig. 19 summarizes the results on the paths with queueing. Nimbus obtained similar throughput to Cubic and 10% lower than BBR but at significantly lower delay (40-50 ms lower than BBR) on these paths.

## 5.8 How General Is Mode-Switching?

We hypothesize that explicit mode-switching is a useful building block: a mode-switching algorithm can use a variety of congestion control algorithms for its DS and TCP-competitive modes, switching using our elasticity detection method. We have implemented Cubic, Reno, and MulTCP [8] as competitive-mode algorithms, and Nimbus delay, Vegas, FAST [37], and COPA [1] as delay-mode algorithms. In Fig. 20, we illustrate two combinations of delay and competitive mode algorithms sharing a bottleneck link with synthetic elastic and inelastic cross-traffic active at different periods during the experiment. The fair-share rate over time is shown as a reference. Both Reno+Nimbus-delay-mode (Fig. 20a) and Cubic+COPA (Fig. 20b) achieve their fair share rate while keeping the delays low in the absence of elastic cross-traffic.

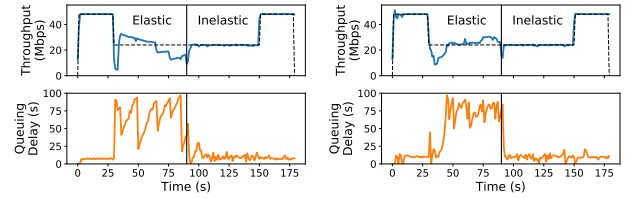


**Figure 20: Explicit mode-switching algorithms combining DS and TCP-competitive algorithms in ways different from Nimbus.**

## 5.9 Limitations

Our method detects only ACK-clocked flows as elastic, not rate-based ones. Almost all traffic today uses ACK-clocking, but a notable exception is BBR [6], which uses both a rate and a congestion window. Nimbus detects BBR only when they are window-limited.

Our techniques assume the flow has a single bottleneck link (§2). Multiple bottlenecks can add noise to Nimbus’s rate measurements, preventing accurate cross-traffic estimation. The challenge is that the spacing of packets at one bottleneck is not preserved when traversing the second bottleneck. Our method will also not work well for RTTs over 300 ms because the background traffic itself may start to vary significantly over that time-scale.

## 6 RELATED WORK

BBR [6] maintains estimates of the bottleneck bandwidth ( $b$ ) and minimum propagation delay ( $d$ ). It paces traffic at a rate  $b$  while keeping  $b \times d$  packets in flight. The presence of other loss-based algorithms sharing the bottleneck buffer inflates BBR’s delay estimate,  $d$ . Depending on the bottleneck buffer size, either the BBR-induced losses limit the throughput of the other TCP flows, or BBR’s delay probing reduces its in-flight data, resulting in lower throughput for BBR itself [5].

Vegas [3], FAST [37], and Copa [1] all aim to maintain a bounded number of packets in the bottleneck queue using different control rules. TCP Nice [36] and LEDBAT [33] are delay-based algorithms to use spare bandwidth without hurting “foreground” transfers. Timely [27] is a designed

for RDMA in datacenters. Other than Copa, these schemes perform poorly when competing with buffer-filling algorithms. Copa has a mechanism to switch into a TCP-competitive mode, but it relies on low-level properties of the dynamics of Copa and does not generalize.

The multiple-Nimbus scheme for coordinating pulsers bears resemblance to receiver-driven layered multicast (RLM) congestion control [26]. In RLM, a sender announces to the multicast group that it is conducting a probe experiment at a higher rate, so any losses incurred during the experiment should not be heeded by the other senders. By contrast, in Nimbus, there is no explicit coordination channel, and the pulsers and watchers coordinate via their independent observations of cross traffic patterns.

## 7 CONCLUSION

This paper showed a method for detecting the elasticity of cross traffic and showed that it is a useful building block for congestion control. The detection technique uses a carefully constructed asymmetric sinusoidal pulse and observes the frequency response of cross traffic rates at a sender. We presented several controlled experiments to demonstrate its robustness and accuracy.

Elasticity detection enables protocols to combine the best aspects of delay-sensitive and buffer-filling algorithms. When cross traffic is buffer-filling, delay-sensitive protocols suffer; but with elasticity detection, a protocol can explicitly switch to a mode that competes well with such cross traffic. And when cross traffic is found to be inelastic, the protocol can revert to delay-sensitive mode, maintaining throughput but at lower queueing delay than a buffer-filling scheme.

We found that our proposed methods are beneficial not only on a variety of emulated conditions that model realistic workloads, but also on a collection of 25 real-world Internet paths.

## REFERENCES

- [1] V. Arun and H. Balakrishnan. Copa: Congestion Control Combining Objective Optimization with Window Adjustments. In *NSDI*, 2018.
- [2] H. Balakrishnan, N. Dukkkipati, N. McKeown, and C. J. Tomlin. Stability analysis of explicit congestion control protocols. *IEEE Communications Letters*, 11(10), 2007.
- [3] L. S. Brakmo, S. W. O'Malley, and L. L. Peterson. TCP Vegas: New Techniques for Congestion Detection and Avoidance. In *SIGCOMM*, 1994.
- [4] CAIDA. The CAIDA Anonymized Internet Traces 2016 Dataset - 2016-01-21. [http://www.caida.org/data/passive/passive\\_2016\\_dataset.xml](http://www.caida.org/data/passive/passive_2016_dataset.xml), 2016.
- [5] N. Cardwell, Y. Cheng, C. S. Gunn, S. H. Yeganeh, and V. Jacobson. BBR Congestion Control. <https://www.ietf.org/proceedings/97/slides/slides-97-icrg-bbr-congestion-control-02.pdf>.
- [6] N. Cardwell, Y. Cheng, C. S. Gunn, S. H. Yeganeh, and V. Jacobson. BBR: Congestion-Based Congestion Control. *ACM Queue*, 14(5):50:20–50:53, Oct. 2016.
- [7] Restructuring Endpoint Congestion Control. SIGCOMM 2018 submission.
- [8] J. Crowcroft and P. Oechslein. Differentiated End-to-end Internet Services Using a Weighted Proportional Fair Sharing TCP. *SIGCOMM CCR*, 28(3):53–69, July 1998.
- [9] M. Dong, Q. Li, D. Zarchy, P. B. Godfrey, and M. Schapira. PCC: Re-architecting Congestion Control for Consistent High Performance. In *NSDI*, 2015.
- [10] C. Dovrolis, P. Ramanathan, and D. Moore. What do packet dispersion techniques measure? In *INFOCOM*. IEEE, 2001.
- [11] A. B. Downey. Using pathchar to estimate internet link characteristics. In *ACM SIGCOMM Computer Communication Review*, volume 29, pages 241–250. ACM, 1999.
- [12] W. Feller. *An introduction to probability theory and its applications*, volume 2. John Wiley & Sons, 2008.
- [13] S. Floyd and V. Jacobson. Random Early Detection Gateways for Congestion Avoidance. *IEEE/ACM Trans. on Networking*, 1(4):397–413, 1993.
- [14] J. Gettys and K. Nichols. Bufferbloat: Dark Buffers in the Internet. *ACM Queue*, 9(11):40, 2011.
- [15] M. Hock, R. Bless, and M. Zitterbart. Experimental Evaluation of BBR Congestion Control. In *ICNP*, 2017.
- [16] J. C. Hoe. Improving the Start-up Behavior of a Congestion Control Scheme for TCP. In *SIGCOMM*, 1996.
- [17] C. V. Hollot, V. Misra, D. Towsley, and W.-B. Gong. On Designing Improved Controllers for AQM Routers Supporting TCP Flows. In *INFOCOM*, 2001.
- [18] N. Hu and P. Steenkiste. Estimating available bandwidth using packet pair probing. Technical report, DTIC Document, 2002.
- [19] V. Jacobson. Pathchar: A tool to infer characteristics of internet paths, 1997.
- [20] D. Katabi, M. Handley, and C. Rohrs. Congestion Control for High Bandwidth-Delay Product Networks. In *SIGCOMM*, 2002.
- [21] C. Kreibich, N. Weaver, B. Nechaev, and V. Paxson. Netalyzr: Illuminating the Edge Network. In *IMC*, 2010.
- [22] S. Kunniyur and R. Srikant. Analysis and design of an adaptive virtual queue (AVQ) algorithm for active queue management. In *SIGCOMM*, 2001.
- [23] K. Lai and M. Baker. Measuring link bandwidths using a deterministic model of packet delay. In *ACM SIGCOMM Computer Communication Review*, volume 30, pages 283–294. ACM, 2000.
- [24] K. Lai and M. Baker. Nettimer: A tool for measuring bottleneck link bandwidth. In *USITS*, volume 1, pages 11–11, 2001.
- [25] B. Mar. pchar: A tool for measuring internet path characteristics. <http://www.employees.org/~bmah/Software/pchar/>, 2000.
- [26] S. McCanne, V. Jacobson, and M. Vetterli. Receiver-driven Layered Multicast. In *SIGCOMM*, 1996.
- [27] R. Mittal, V. T. Lam, N. Dukkkipati, E. Blem, H. Wassel, M. Ghobadi, A. Vahdat, Y. Wang, D. Wetherall, and D. Zats. TIMELY: RTT-based Congestion Control for the Datacenter. In *SIGCOMM*, 2015.
- [28] A. Narayan, F. Cangialosi, P. Goyal, S. Narayana, M. Alizadeh, and H. Balakrishnan. The Case for Moving Congestion Control Out of the Datapath. In *HotNets*, 2017.
- [29] R. Netravali, A. Sivaraman, S. Das, A. Goyal, K. Winstein, J. Mickens, and H. Balakrishnan. Mahimahi: Accurate Record-and-Replay for HTTP. In *USENIX Annual Technical Conference*, 2015.
- [30] K. Nichols and V. Jacobson. Controlling Queue Delay. *ACM Queue*, 10(5), May 2012.
- [31] R. Pan, P. Natarajan, C. Piglion, M. Prabhu, V. Subramanian, F. Baker, and B. VerSteeg. PIE: A lightweight control scheme to address the bufferbloat problem. In *Intl. Conf. on High Performance Switching and Routing (HPSR)*, 2013.
- [32] D. Rossi, C. Testa, S. Valenti, and L. Muscariello. Ledbat: The new bittorrent congestion control protocol. In *ICCCN*, pages 1–6, 2010.

- [33] S. Shalunov, G. Hazel, J. Iyengar, and M. Kuehlewind. Low Extra Delay Background Transport (LEDBAT), 2012. RFC 6817, IETF.
- [34] K. Tan, J. Song, Q. Zhang, and M. Sridharan. A Compound TCP Approach for High-speed and Long Distance Networks. In *INFOCOM*, 2006.
- [35] A. Tirumala, F. Qin, J. Dugan, J. Ferguson, and K. Gibbs. Iperf: The TCP/UDP bandwidth measurement tool. <http://dast.nlanr.net/Projects>, 2005.
- [36] A. Venkataramani, R. Kokku, and M. Dahlin. TCP Nice: A Mechanism for Background Transfers. In *OSDI*, 2002.
- [37] D. Wei, C. Jin, S. Low, and S. Hegde. FAST TCP: Motivation, Architecture, Algorithms, Performance. *IEEE/ACM Trans. on Networking*, 14(6):1246–1259, 2006.
- [38] K. Winstein, A. Sivaraman, and H. Balakrishnan. Stochastic Forecasts Achieve High Throughput and Low Delay over Cellular Networks. In *NSDI*, 2013.